Journal of Molecular Structure 991 (2011) 60–67

Contents lists available at ScienceDirect

Journal of Molecular Structure

journal homepage: www.elsevier.com/locate/molstruc

Study of thermal and electrical properties exhibited by two ferroelectric self assembly systems

V.N. Vijayakumar, M.L.N. Madhu Mohan *

Liquid Crystal Research Laboratory (LCRL), Bannari Amman Institute of Technology, Sathyamangalam 638 401, India

ARTICLE INFO

Article history:
Received 2 December 2010
Received in revised form 30 January 2011
Accepted 31 January 2011
Available online 24 February 2011

Keywords:
Ferroelectric self assembly systems
Thermal and electrical characterization
Dielectric relaxation
Activation energies
DSC
FTIR

ABSTRACT

Two series of inter hydrogen bonded ferroelectric liquid crystals have been isolated. In one of the series hydrogen bond is formed between p-*n*-alkyloxy benzoic acids and (S)-1,2-cholo-3-(4-hydroxy) phenyl propionic acid (CTy + *n*OBA) while in the other it is formed between p-*n*-alkyl benzoic acids and (S)-1,2-cholo-3-(4-hydroxy) phenyl propionic acid (CTy + *n*BA). Detailed synthetic route for the isolation of these compounds is discussed. Formation of the ferroelectric self assembly systems has been evinced through FTIR studies. The positional influence of oxygen atom is investigated from the thermal and electrical characterization of both the series. Polarizing optical microscope (POM) studies on CTy + *n*BA hydrogen bonded complexes reveals that they exhibit single phase variance while the other complex CTy + *n*OBA exhibit rich phase polymorphism. It is observed that the presence of oxygen atom enhances phase abundance. Phase diagrams for both the complexes are constructed from the DSC and POM studies. Dielectric relaxations and activation energies have been carried out for various phases in CTy + 8OBA and CTy + 8BA complexes. It has been observed that the oxygen atom originates type I relaxation process. Two molecular modeling have been assigned to account for the dielectric relaxation process observed in both the HBFLC series.

1. Introduction

Since the discovery of first ferroelectric liquid crystal by Meyer [1] interest on these soft materials have grown enormously. In recent times hydrogen bonded ferroelectric liquid crystals [HBFLC] reported [2–14] in literature are designed and synthesized from materials selected on the basis of their molecular reorganization and self assembly capability. The applicational aspects [15–18], and commercial viabilities made many research groups to work on these hydrogen bonded ferroelectric liquid crystals.

Hydrogen bonded liquid crystalline materials are known since early 1960s [3,4], however in the recent times [5–13,18–21] much work has been done on these complexes. Hydrogen bond enables various mesogenic and non mesogenic compounds to form complexes which exhibit rich phase polymorphism. HBFLC usually are composed of a proton donor and acceptor molecules. The reported data [5–12,18–22] indicates the fact that if an HBLC material to be mesogenic it is enough either one of proton donor or an acceptor molecules exhibits mesogenic property. The chemical molecular structure [10,18–22] of HBFLC is co-related to the physical properties exhibited by it. The reported literature suggests the formation of HBFLC through carboxylic acids as well as from mixtures of unlike molecules capable of interacting through H-bonding [13–21]. Usually in all these HBLC the rigid core is made up of covalent and non covalent hydrogen bonding. With our previous experience [23–30], in designing, synthesizing and characterizing various types of liquid crystals, a successful attempt has been made in characterizing a novel series of inter hydrogen bonded ferroelectric liquid crystal.

In the present communication a homologous series of HBFLC is designed in such a way that the molecule possesses a chiral center and the hydrogen bonding is on one side of the chiral centre moiety. (S)-1,2-cholo-3-(4-hydroxy) phenyl propionic acid is the ferroelectric ingredient, formed hydrogen bond with mesogenic p-*n*-alkyloxy benzoic acid respectively. Thermal and electrical characterization of three HFBLC complexes of the present series is discussed in detail.

2. Experimental

Optical textural observations were made with a Nikon polarizing microscope equipped with Nikon digital CCD camera system with 5 mega pixels and 2560 × 1920 pixel resolutions. The liquid crystalline textures are processed, analyzed and stored with the aid of ACT-2U imaging software system. The temperature control of the liquid crystal cell is equipped by Instec HCS402-STC 200 temperature controller (Instec, USA) to a temperature resolution

* Corresponding author. Tel.: +91 9442437480; fax: +91 4295 223 775.
E-mail address: mln.madhu@gmail.com (M.L.N. Madhu Mohan).

0022-2860/$ - see front matter © 2011 Elsevier B.V. All rights reserved.
doi:10.1016/j.molstruc.2011.01.068

of 0.1 °C. This unit is interfaced to computer by IEEE-STC 200 to control and monitored the temperature. The liquid crystal sample is filled by capillary action in its isotropic state into a commercially available (Instec, USA) polyamide buffed cell with 4 μm spacer. Optical extinction technique is used for the determination of tilt angle. The transition temperatures and corresponding enthalpy values are obtained by DSC (Shimadzu DSC-60). FTIR spectra is recorded (ABB FTIR MB3000) and analyzed with the MB3000 software. For dielectric studies Agilent HP4192A LF impedance analyzer is used. The p-*n*-alkyloxy benzoic acids, p-*n*-alkyl benzoic acids and (S)-2-amino-3-(4-hydroxy)phenyl propionic acid are supplied by Sigma Aldrich, Germany and all the solvents used are E.Merk grade.

2.1. Synthesis of HBFLC

The synthetic route for preparation of (S)-1,2-cholo-3-(4-hydroxy) phenyl propionic acid is given as Schemes 1a and 1b while a detailed synthetic procedure including various intermediates is presented below.

(S)-1,2-cholo-3-(4-hydroxy)phenyl propionic acid [1] is prepared by dissolving (S)-2-amino-3-(4-hydroxy)phenyl propionic acid (5.43 g, 30.0 mmol) in 20 cm^3 of 6 N HCl and bringing the solution between 0 °C and 5 °C. Freshly pulverized sodium nitrite (2.72 g, 32.0 mmol) is added to the solution in small portions with vigorous stirring while maintaining the reaction temperatures between 0 °C and 5 °C. The reaction mixture is stirred for 12 h and then extracted with 40 cm^3 of diethyl ether. The ethereal layer is dried over anhydrous sodium sulfate for 12 h. The crude product, obtained as yellow on removing the excess solvent by distillation under reduced pressure, is washed repeatedly with cold EtOH and finally recrystallized from hot dichloromethane to get 55% yield.

Intermolecular hydrogen bonded ferroelectric mesogens are synthesized as depicted in Scheme 1a, by the addition of one mole of p-*n*-alkyloxy benzoic acids (*n*OBA, where *n* = 5, 6, 7 and 8) with one mole of above synthesized (S)-1,2-cholo-3-(4-hydroxy)phenyl propionic acid in N,N-Dimethyl formamide (DMF) respectively. The other hydrogen bonded complex is prepared as shown in Scheme 1b, by the addition of one mole of p-*n*-alkyl benzoic acids (*n*BA, where *n* = 3, 5, 7 and 8) with one mole of above synthesized (S)-1,2-cholo-3-(4-hydroxy)phenyl propionic acid in N,N-Dimethyl formamide (DMF) respectively. Further they are subject to constant stirring for 12 h at ambient temperature of 30 °C till a precipitate in a dense solution is formed. The white crystalline crude complexes so obtained by removing excess DMF are then recrystallized with Dimethyl Sulfoxide (DMSO) and the yield varied from 85% to 95%. Yield of higher homologs complexes are observed to be more compared to its lower counterparts. Similar procedure is adopted for the synthesis of intermolecular hydrogen bonded ferroelectric liquid crystal pertaining to p-*n*-alkyl benzoic acids (*n*BA, where *n* = 3, 5, 7 and 8). The molecular structure of the ferroelectric hydrogen bonded complex CTy + *n*OBA and CTy + *n*BA are separately shown as Figs. 1 and 2 respectively.

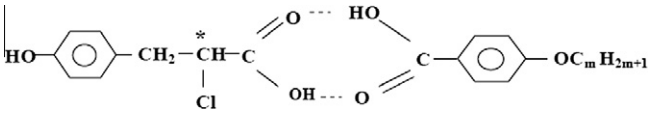

Fig. 1. Molecular structure of CTy + *n*OBA HBFLC.

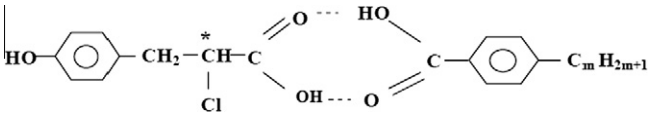

Fig. 2. Molecular structure of CTy + *n*BA HBFLC.

3. Results and discussion

All the mesogens isolated under the present investigation are pale yellow crystalline solids and are stable at room temperature.

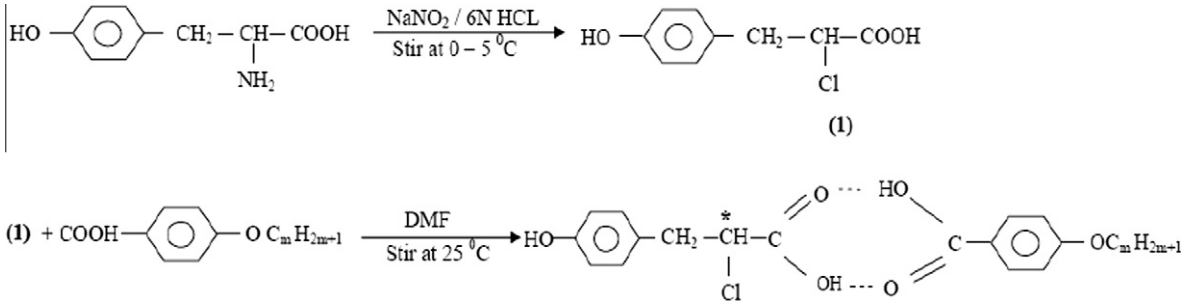

Scheme 1a. Synthesis route of CTy + *n*OBA hydrogen bonded ferroelectric complexes.

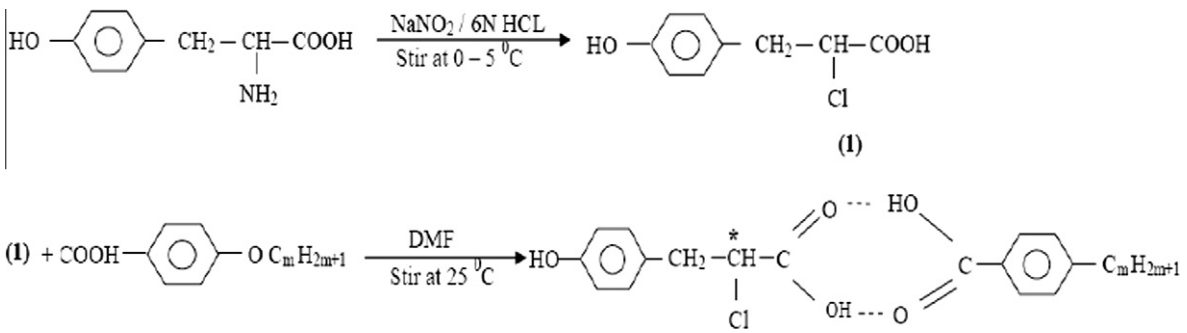

Scheme 1b. Synthesis route of CTy + *n*BA hydrogen bonded ferroelectric complexes.

Table 1
Comparison of various phase transition temperatures of CTy + *n*OBA homologous series obtained by different techniques. Enthalpy values in J/g obtained from DSC studies are given in parenthesis.

Carbon	Phase variance	Technique	Crystal to melt	Ch	C*	F*	G*	Crystal
5	F*	DSC (h)	120.6 (73.18)			#		
		DSC (c)				112.4 (Merged with crystal)		107.9 (16.28)
		POM (C)				112.8		108.5
6	Ch F*	DSC (h)	103.9 (27.71)	#		#		
		DSC (c)		104.4 (0.95)		91.1 (1.76)		90.0 (6.11)
		POM (C)		104.8		91.9		92.1
7	Ch F*	DSC (h)	92.4 (51.08)	#		#		
		DSC (c)		84.2 Merged with F		83.5 (23.18)		67.6 (26.07)
		POM (C)		84.6		83.9		
8	Ch C* G*	DSC (h)	75.8 (27.74)	#	99.7 (1.63)		88.4 (0.39)	
		DSC (c)		131.1 (0.27)	92.4 (2.45)		90.1 (11.82)	52.1 (22.22)
		POM (C)		131.5	92.9		90.5	52.6

Monotropic transition.

Table 2
Comparison of various phase transition temperatures of CTy + *n*BA homologous series obtained by different techniques. Enthalpy values in J/g obtained from DSC studies are given in parenthesis.

Carbon	Phase variance	Technique	Crystal to melt	G*	Crystal
3	G*	DSC (h)	130.6 (5.12)	#	
		DSC (c)		113.3 (Merged with crystal)	117.6 (19.25)
		POM (c)		113.7	118.1
5	G*	DSC (h)	85.3 (5.09)	#	
		DSC (c)		79.2 (Merged with crystal)	76.0 (18.18)
		POM (c)		79.7	76.4
7	G*	DSC (h)	96.9 (30.15))	#	
		DSC (c)		90.8 (Merged with crystal)	88.4 (26.79)
		POM (c)		91.3	88.7
8	G*	DSC (h)	90.4 (35.04)	#	
		DSC (c)		86.9 (Merged with crystal)	85.0 (35.68)
		POM (c)		87.3	88.4

Monotropic transition.

They are insoluble in water and sparingly soluble in common organic solvents such as methanol, ethanol, and benzene and dichloromethane. However they show a high degree of solubility in coordinating solvents like Dimethyl Sulfoxide (DMSO), Dimethyl formamide (DMF) and pyridine. All these mesogens under present investigation melt at specific temperatures below 150 °C (Tables 1 and 2). They show high thermal and chemical stability when subjected to repeated thermal scans performed during polarizing optical microscopic (POM) and DSC studies.

3.1. Polarizing optical microscopic studies (POM)

The mesogens of the (S)-1,2-cholo-3-(4-hydroxy)phenyl propionic acid and alkyloxy benzoic acid (CTy + *n*OBA) and (S)-1,2-cholo-3-(4-hydroxy)phenyl propionic acid and alkyl benzoic acid (CTy + *n*BA) ferroelectric homologous series are found to exhibit characteristic textures [31], viz., Cholesteric (schlieren texture) (Plate 1), Smectic C* (broken focal conic texture) Smectic F* (chequered board texture and Smectic G* (multi colored mosaic texture) respectively. The general phase sequence pertaining to CTy + *n*OBA and CTy + *n*BA homologous series can be shown as

$$\text{Isotropic} \rightarrow \text{Sm F}^* \rightarrow \text{Crystal} \quad \text{CTy} + 5\text{OBA}$$
$$\text{Isotropic} \rightarrow \text{Ch} \rightarrow \text{Sm F}^* \rightarrow \text{Crystal} \quad \text{CTy} + 6\text{OBA}, \text{CTy} + 7\text{OBA}$$
$$\text{Isotropic} \rightarrow \text{Ch} \rightarrow \text{Sm C}^* \rightarrow \text{Sm G}^* \rightarrow \text{Crystal} \quad \text{CTy} + 8\text{OBA}$$
$$\text{Isotropic} \rightarrow \text{Sm G}^* \rightarrow \text{Crystal} \quad \text{CTy} + n\text{BA} \ (n = 3, 5, 7, 8)$$

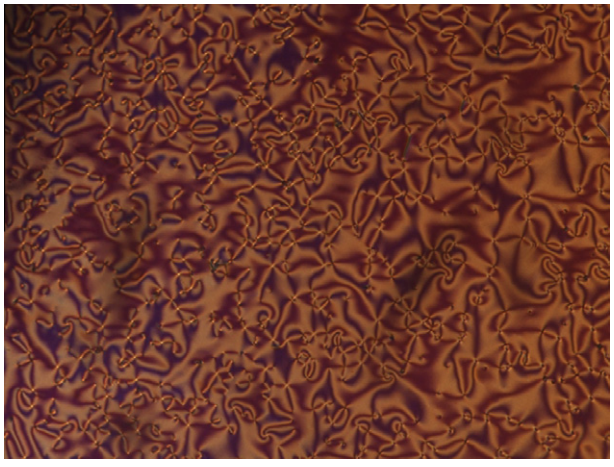

Plate 1. Schlieren texture of cholesteric in CTy + 8OBA complex.

3.2. Infrared spectroscopy (FTIR)

IR spectra of free p-*n*-alkyloxy benzoic acid, (S)-1,2-cholo-3-(4-hydroxy) phenyl propionic acid and their intermolecular ferroelectric self assembly systems are recorded in the solid state (KBr) at room temperature. Fig. 3 illustrates the FTIR spectra of the hydrogen bonded complex of (S)-1,2-cholo-3-(4-hydroxy) phenyl

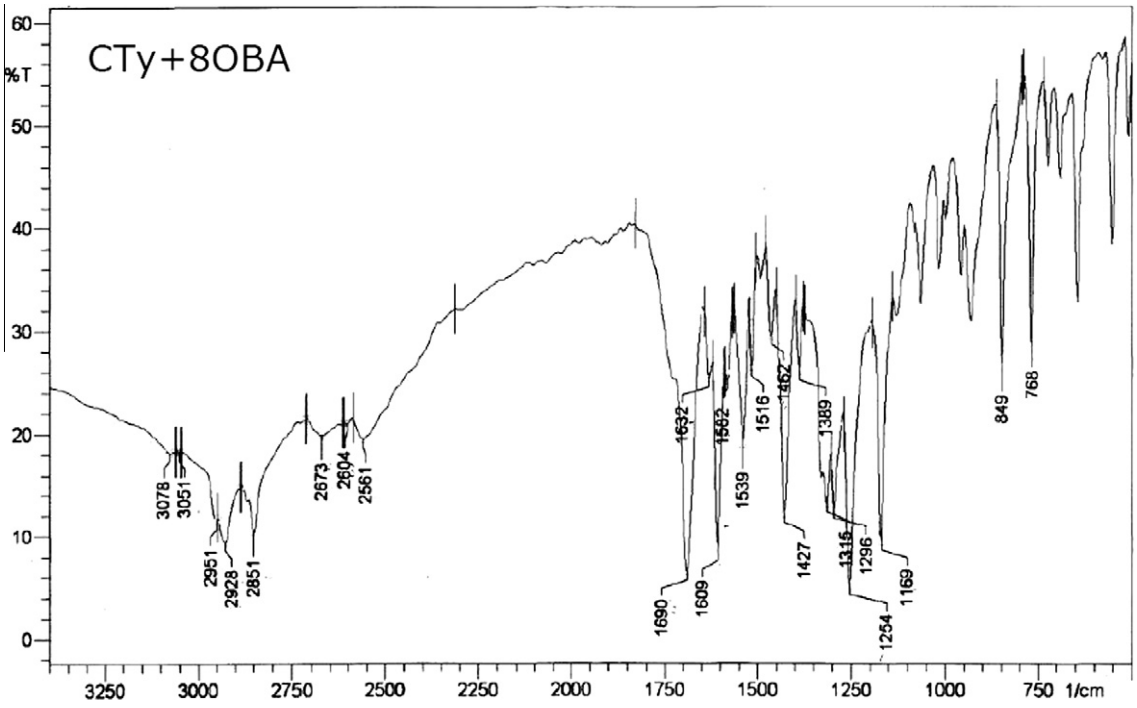

Fig. 3. FTIR of CTy + 8OBA complex.

propionic acid with octyloxy benzoic acid (CTy + 8OBA) in solid state at room temperature while Fig. 4 represents the FTIR spectra of hydrogen bonded complex of (S)-1,2-cholo-3-(4-hydroxy) phenyl propionic acid with octyl benzoic (CTy + 8BA), as a representative case. The solid state spectra of free alkyloxy benzoic acid is reported [21] to have two sharp bands at 1685 cm^{-1} and 1695 cm^{-1} due to the frequency ν(C=O) mode. The doubling feature of this stretching mode confirms the dimeric nature of alkyloxy benzoic acid at room temperature [21]. Further in the present hydrogen bonded complexes a band appearing at 2928 cm^{-1} and 2924 cm^{-1} pertaining to CTy + 8OBA, CTy + 8BA respectively is assigned to ν (O–H) mode of the carboxylic acid group. Moreover, in the present hydrogen bonded complex, a sharp intense band at 768 cm^{-1} and 760 cm^{-1} pertaining to CTy + 8OBA, CTy + 8BA respectively are attributed to the ν(C–Cl) stretching mode.

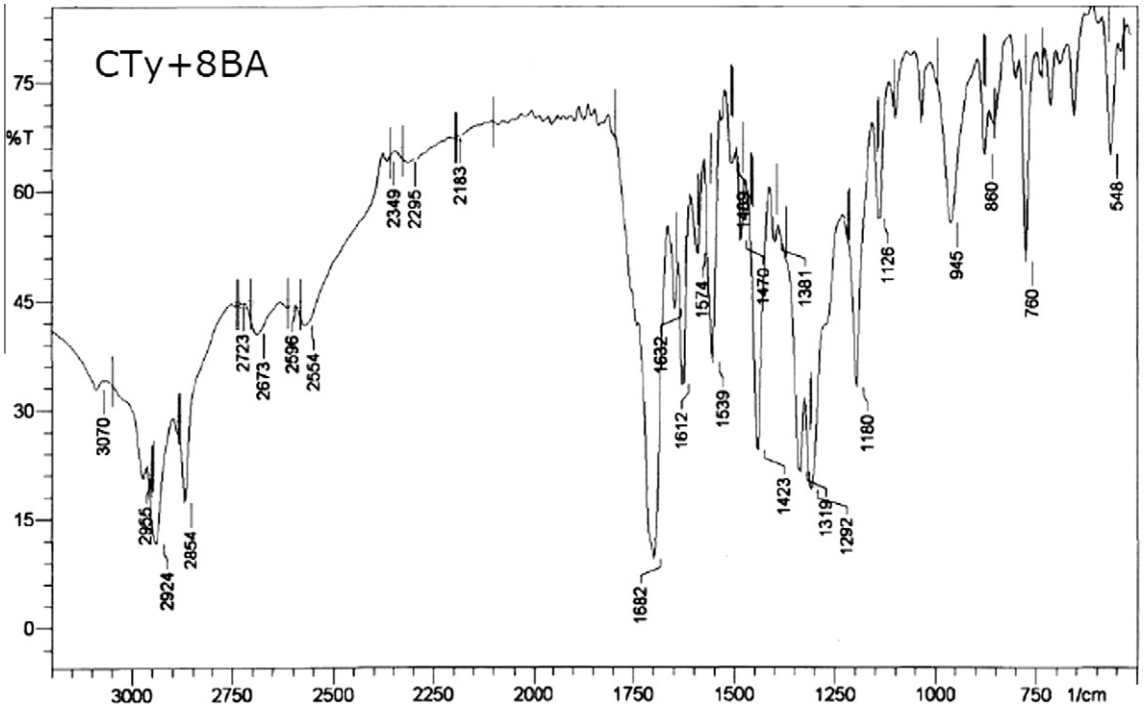

Fig. 4. FTIR of CTy + 8BA complex.

The doubling nature of ν(C=O) mode may be attributed to the dimeric nature of acid group at room temperature [21]. Corresponding spectrum of solution state (chloroform) shows a strong intense band suggesting the existence of monomeric form of benzoic acid. A noteworthy feature in the spectra of the present complex is the appearance of the sharp band at 1258 cm^{-1} and non appearance of the doubling nature of ν(C=O) mode of benzoic acid moiety. This clearly suggests that the dimeric nature of the benzoic acid dissociates and prefers to exist in a monomeric form upon complexation. Further the presence of an intense peak at 1516 cm^{-1} in the CTy + 8OBA and the absence of the same peak in corresponding hydrogen bonded complex of CTy + 8BA confirms the skeletal vibrations of the above hydrogen bonded complex aromatic system.

3.3. DSC studies

DSC thermograms are obtained in heating and cooling cycle. The sample is heated with a scan rate of 10 °C/min and hold at its isotropic temperature for one minute so as to attain thermal stability. The cooling run is performed with a scan rate of 10 min/°C. The respective equilibrium transition temperatures and corresponding enthalpy values of the mesogens of the homologous series are listed separately in Table 1. Cholesteric phase in the compounds CTy + 7OBA, CTy + 8OBA and smectic F* phase in CTy + 6OBA, CTy + 7OBA are observed to be monotropic transitions in the DSC heating run. Fig. 5a illustrates the DSC thermogram of CTy + 8BA hydrogen bonded complex. Smectic G* phase which is merged with crystal is depicted in the thermogram. Fig. 5b illustrates the DSC thermogram of CTy + 8OBA. From these two thermograms it is evident that a cluster of new phases are induced by interdiction of oxygen atom in the parent sample. Table 2 elucidates the CTy + *n*BA series enthalpy values and transition temperatures obtained by DSC and POM studies. Interestingly it is observed that all the complexes of this series exhibit a monotropic transition of smectic G* in the heating run.

3.4. Phase diagram of pure p-n-alkyloxy benzoic acids

The phase diagrams of pure p-*n*-alkyloxy benzoic acids is reported [24] while the present hydrogen bonded ferroelectric homologous series is constructed through optical polarizing microscopic studies and by the phase transition temperatures observed in the cooling run of the DSC thermogram. The phase diagram of

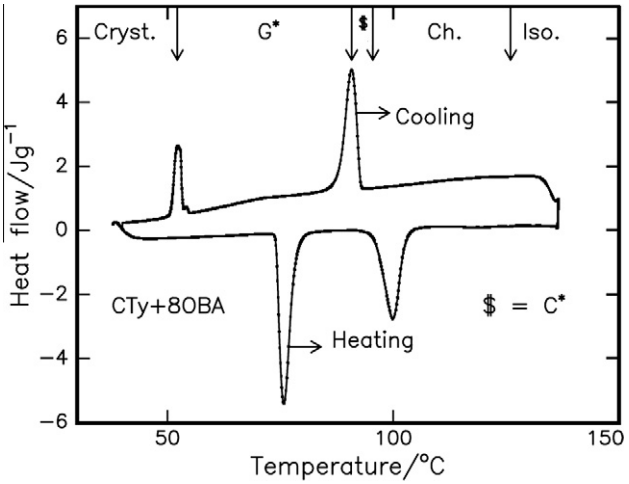

Fig. 5a. DSC thermogram of CTy + 8OBA.

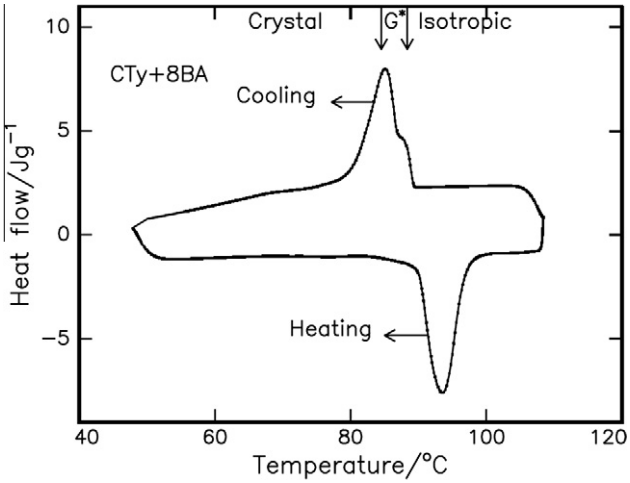

Fig. 5b. DSC thermogram of CTy + 8BA.

pure p-*n*-alkyloxy benzoic acid is reported [24] to composed of three phases namely, Nematic, smectic C* and smectic G*.

3.5. Phase diagram of CTy + nOBA homologous series

The phase diagrams of the present hydrogen bonded ferroelectric homologous series are depicted in Fig. 6. The following points can be observed from the Fig. 6

(a) The mesogenic range gradually increased with increment in the alkyloxy carbon number from pentyloxy to dodecyloxy benzoic acid.
(b) The homologous series exhibits rich phase abundance, the number of phases exhibited by the individual member's increases as the carbon number is increased up to octyloxy benzoic acid.
(c) In the last members of the series namely octyloxy benzoic acid the phase variance stabilized to three phases viz, Ch C* G*.
(d) In the lower homologous members of the series, smectic F* is found to be pronounced while in the higher homologous member of the series smectic G* swapped the thermal range of smectic F*.
(e) Compared to the pure benzoic acids, in the binary the thermal span of the three main phases Cholesteric, smectic C* and G* are found to be almost equal.

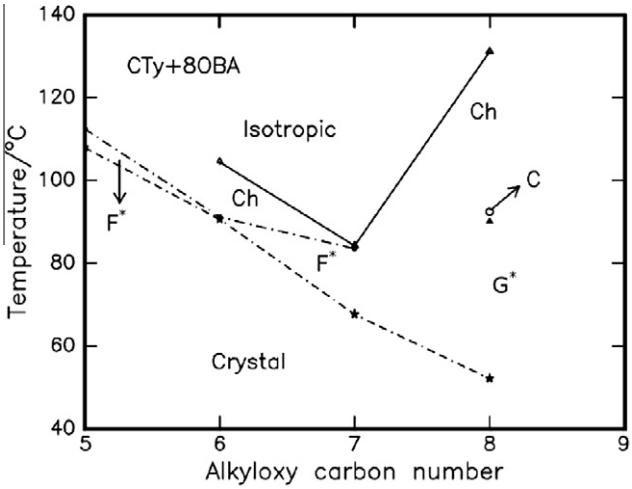

Fig. 6. Phase diagram of CTy + *n*OBA homologous series.

3.6. Phase diagram of CTy + nBA homologous series

The phase diagrams of the present hydrogen bonded ferroelectric homologous series are depicted in Fig. 7. The following points can be observed from the Fig. 7. The following points are observed from the Fig. 7

(a) Entire homologous series exhibits only a single phase viz., smectic G*.
(b) The thermal span of the smectic G* phase is almost unaltered with the increment in the alkyl carbon number from 3 to 8.
(c) The isotropic temperatures steeply reduced from 117 °C in propyl hydrogen bonded complex to 87 °C in octyl hydrogen bonded complex.
(d) In the entire homologous series, the isotropic and crystal temperatures ran parallel to each other.

3.7. Optical tilt angle studies

For the hydrogen bonded CTy + 8OBA complex, optical tilt angle has been experimentally measured by optical extinction method [32] in the smectic C* phases. From the Fig. 8 it is observed that the tilt angle increases with decreasing temperature and attains a saturation value of 18°. The large magnitudes of the tilt angle are attributed [22] to the direction of the soft covalent hydrogen bond interaction which spreads along molecular long axis with finite inclination.

Tilt angle is a primary order parameter [32,33] in tilted phases namely smectic C* the temperature variation is estimated by fitting the observed data of $\theta(T)$ to the relation

$$\theta(T)\alpha(T - T_C)^{\beta} \quad (1)$$

The critical exponent β value estimated by fitting the data of $\theta(T)$ to the above Eq. (1) is found to be 0.50 to agree with the Mean Field [34] prediction. The dotted line in the Fig. 8 depicts the fitted data. Further, the agreement of β with Mean Field value infers the long-range interaction of transverse dipole moment for the stabilization of tilted smectic C* phase.

4. Dielectric relaxations

Dielectric dispersion i.e. frequency variation of dielectric loss, are studied at different temperatures in cholesteric, smectic C* smectic F* phases exhibited by CTy + 8OBA while the same has been carried out in smectic F* of CTy + 8BA in the frequency range of 5 Hz–13 MHz. An impedance analyzer (HP4192A) is operated with $1V_{P-P}$ oscillating signal with zero bias field. Relative permittivity $\varepsilon'_r(\omega)$ and dielectric loss $\varepsilon''(\omega)$ are calculated.

To detect the possible relaxation in both the HBFLC complexes, the mesogens are scanned in the frequency range of 5 Hz–13 MHz at different temperatures corresponding to various cholesteric and smectic phases. As a representative case for CTy + 8OBA mesogen exhibits two relaxations at lower and higher end of the frequency spectrum. Two types of relaxation mechanisms namely Type I and Type II relaxation are observed in the cholesteric and smectic G* phases. The corresponding Arrhenius plots are given in Fig. 9. The activation energies are tabulated in Table 3.

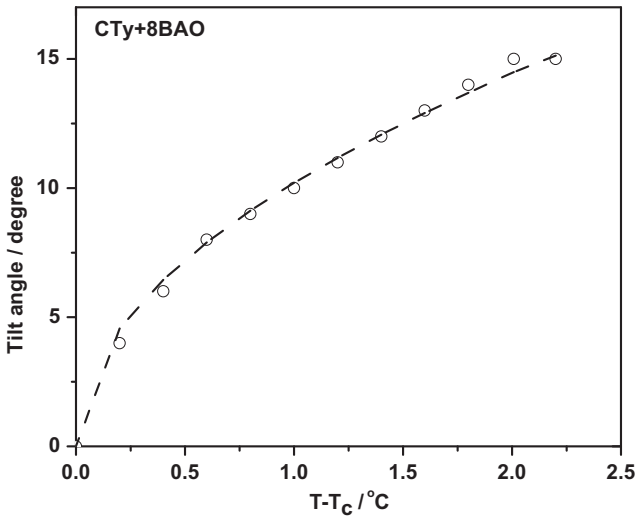

Fig. 8. Temperature variation of tilt angle for CTy + 8OBA complex in the smectic C* phase. Dotted line shows the fitted data.

5. Molecular modeling for CTy + *n*OBA Series

The distinct response of the dipolar orientations evinced experimentally in the present hydrogen bonded ferroelectric series as type I and type II are attributed to the molecular modeling

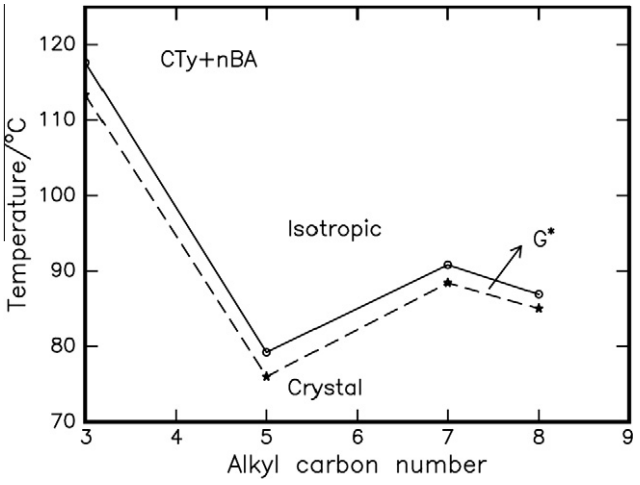

Fig. 7. Phase diagram of CTy + *n*BA homologous series.

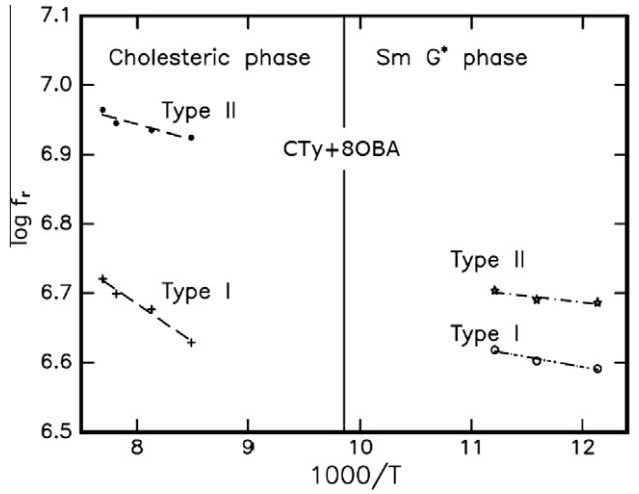

Fig. 9. Arrhenius plots for type I, type II in cholesteric, smectic G* phases of CTy + 8OBA complex.

Table 3
Activation energies (eV) and relaxation frequencies (Hz) obtained in various phases of CTy + *n*OBA and CTy + *n*BA HBFLC complexes.

HBFLC	Phase	Type	Temperature (°C)	Relaxation frequency, f_r (MHz)	Activation energy (eV)
CTy + 8OBA	Cholesteric	Type I	128	5.25	0.11
	G*		85.1	4.15	0.03
	Cholesteric	Type II	128	9.20	0.04
	G*		85.1	5.05	0.02
CTy + 8BA	G*	Type II	86	8.25	0.05

illustrated in Figs. 10a and 10b. The dipole moments are classified into two categories:

The type I relaxation mechanism is attributed to the longitudinal dipole moment (μ_l) situated at the corner of the rigid part of molecule. In the present series this longitudinal dipole moment (μ_1) is observed as the oxygen molecule attached to the benzene core on one side of the molecular structure of HBFLC.

The type II relaxation mechanism is attributed to the longitudinal dipole moment (μ_l) situated at the flexible part of the molecular structure. This is depicted in Fig. 10a as oxygen molecule pertaining to the carbon atom forming the hydrogen bonding frame work. Further this arrangement of the hydrogen bonding permits to have an electronegative oxygen atoms giving arise to type II relaxations.

5.1. Molecular modeling for CTy + nBA series

The molecular modeling for this series is presented in Fig. 10b. In this series because of the absence of oxygen atom attached to the alkyl benzoic carbon, type I relaxation is not observed. However type II relaxation is persistent which has been experimentally evaluated and the data is presented in Table 3.

It is evinced from our dielectric studies related to both the series that longitudinal dipole moment (μ_l) corresponding to the flexible part of the molecular structure is rather slow compared to longitudinal dipole moment (μ_l) situated at the corner of the rigid part of molecule. This result is in good agreement with reported [35–37] HBFLC molecules.

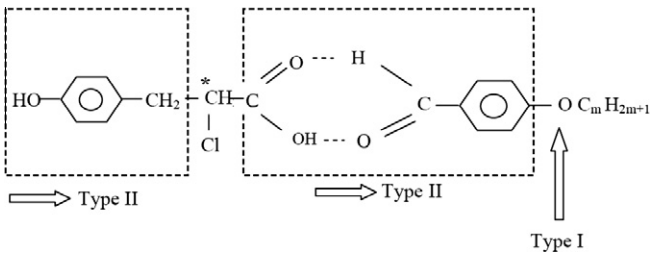

Fig. 10a. Molecular modeling indicating various types of relaxations for CTy + *n*OBA series.

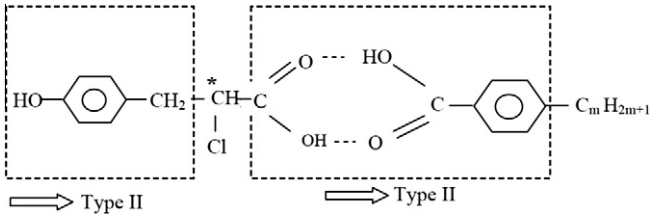

Fig. 10b. Molecular modeling indicating various types of relaxations for CTy + *n*BA series.

6. Conclusions

i. Two novel series of inter hydrogen bonded ferroelectric liquid crystals have been isolated.
ii. The positional influence of oxygen atom has been investigated from the thermal and electrical characterization of both the series.
iii. Dielectric relaxations (Type I and Type II) and activation energies have been carried out for various phases in CTy + 8OBA and CTy + 8BA complexes.

Acknowledgements

The authors acknowledges the financial support rendered by All India Council for Technical Education (AICTE), Department of Science and Technology (DST), and Defence Research Development Organization (DRDO), New Delhi. Infrastructural support provided by Bannari Amman Institute of Technology is gratefully acknowledged.

References

[1] R.B. Meyer, L. Liebert, L. Strezelecki, P. Keller, J. Phys. Lett. 36 (1975) 69.
[2] T. Kato, Handbook of Liquid Crystals, Weinheim, Wiley-VCH, 1998.
[3] G.W. Gray, Molecular Structure and Properties of Liquid Crystals, Academic press, London., 1962.
[4] H. Kelker, R. Hatz, Handbook of Liquid Crystals, Verlag Chemie, Weinheim, 1980.
[5] T. Kato, J.M.J. Frechet, J. Am. Chem. Soc. 111 (1989) 8533.
[6] L. Yu, Liquid Cryst. 14 (1993) 1303.
[7] T. Kato, H. Kihara, T. Uryu, S. Ujiie, K. Iimura, J.M.J. Fréchet, U. Kumar, Ferroelectrics 148 (1993) 161.
[8] T. Kato, T. Uryu, F. Kaneuchi, C. Jin, J.M.J. Fréchet, Liquid Cryst. 14 (1993) 1311.
[9] D. Demus, H. Demus, H. Zaschke, Flussige Kristalle in Tabellen, VEB Deutscher Verlag fur Grundstoffindustrie, Leipzig, 1974.
[10] C.M. Paleos, D. Tsiourvas, Liquid Cryst. 28 (2001) 1127.
[11] B. Xu, T.M. Swager, J. Am. Chem. Soc. 117 (1995) 5011.
[12] S. Malik, P.K. Dhal, R.A. Mashelkar, Macromolecules 28 (1995) 2159.
[13] Z. Sideratou, D. Tsiourvas, C.M. Paleos, A. Skoulios, Liquid Cryst. 22 (1997) 51.
[14] J.W. Goodby, R. Blinc, N.A. Clark, S.T. Lagerwall, S.A. Osipov, S.A. Pikin, T. Sakurai, Ferro Electric Liquid Crystal, Principles, Properties, and Applications, Gorden and Breech Press, Philadalphia, USA, 1991.
[15] N.A. Clark, S.T. Lagerwall, Appl. Phys. Lett. 36 (1980) 899.
[16] H.R. Brand, P.E. Cladis, H. Pleiner, Macromolecules 25 (1992) 7223.
[17] M.P. Petrov, L.V. Tsonev, Liquid Cryst. 21 (1996) 543.
[18] P.A. Kumar, M. Srinivasulu, V.G.K.M. Pisipati, Liquid Cryst. 26 (1999) 859.
[19] P. Swathi, P.A. Kumar, V.G.K.M. Pisipati, Liquid Cryst. 27 (2000) 665.
[20] M. Srinivasulu, P.V.V. Satyanarayana, P.A. Kumar, V.G.K.M. Pisipati, Liquid Cryst. 28 (2001) 1321.
[21] P. Swathi, S. Sreehari Sastry, P.A. Kumar, V.G.K.M. Pisipati, Mol. Cryst. Liquid Cryst. 365 (2001) 523.
[22] B. Sreedevi, P.V. Chalapathi, M. Srinivasulu, V.G.K.M. Pisipati, D.M. Potukuchi, Liquid Cryst. 31 (2004) 303.
[23] T. Chitravel, M.L.N. Madhu Mohan, V. Krishnakumar, Mol. Cryst. Liquid Cryst. 493 (2008) 17;
V.N. Vijayakumar, K. Murugadass, M.L.N. Madhu Mohan, Mol. Cryst. Liquid Cryst. 515 (2010) 37.
[24] V.N. Vijayakumar, K. Murugadass, M.L.N. Madhu Mohan, Mol. Cryst. Liquid Cryst. 517 (2010) 41;
V.N. Vijayakumar, M.L.N. Madhu Mohan, Solid State Commun. 149 (2009) 2090;
V.N. Vijayakumar, K. Murugadass, M.L.N. Madhu Mohan, Braz. J. Phys. 39 (2009) 600.
[25] M.L.N. Madhu Mohan, B. Arunachalam, C. Arravindh Sankar, Metal Mater. Trans. A 39 (2008) 1192;
M.L. N Madhu Mohan, B. Arunachalam, Z .Naturforch 63a (2008) 435.
[26] M.L.N. Madhu Mohan, V.G.K.M. Pisipati, Liquid Cryst. 26 (2000) 1609.
[27] P.A. Kumar, M.L.N. Madhu Mohan, V.G.K.M. Pisipati, Liquid Cryst. 27 (2000) 1533.
[28] M.L.N. Madhu Mohan, P.A. Kumar, B.V.S. Goud, V.G.K.M. Pisipati, Mater. Res. Bull. 34 (1999) 2167.
[29] M.L.N. Madhu Mohan, P.A. Kumar, V.G.K.M. Pisipati, Ferroelectrics 227 (1999) 105;
V. N. Vijayakumar, M. L. N. Madhu Mohan, Mol. Cryst. Liq. Cryst., accepted for publication.

[30] V.N. Vijayakumar, M.L.N. Madhu Mohan, Integr. Ferroelectr. 392 (2009) 81; V.N. Vijayakumar, K. Murugadass, M.L.N. Madhu Mohan, Mol. Cryst. Liquid Cryst. 517 (2010) 111.
[31] G.W. Gray, J.W.G. Goodby, Smetic Liquid Crystals – Textures and Structures, Leonard Hill, London, 1984.
[32] C. Noot, S.P. Perkins, H.J. Coles, Ferroelectrics 244 (2000) 331.
[33] P.G. de Gennes, The Physics of Liquid Crystals, Oxford Press, London, 1974.
[34] H.E. Stanley, Introduction to Phase Transition and Critical Phenomena, Clarendon Press, 1971.
[35] F. Gouda, K. Skarp, S.T. Lagerwall, Ferroelectrics 113 (1991) 165.
[36] D.M. Potukuchi, B.V.S. Goud, V.G.K.M. Pisipati, Ferroelectrics 289 (2002) 77.
[37] B. Sreedevi, P.V. Chalapathi, V.K.M. Kotikalapudi, V.G.K.M. Pisipati, D.M. Potukuchi, Ferroelectrics 361 (2007) 18.